JOURNAL OF MAGNETIC RESONANCE **126,** 1–8 (1997)
ARTICLE NO. MN971135

Studies of an Isolated $^{15}N-^{15}N$ Spin Pair. Off-Angle Fast-Sample-Spinning NMR and Self-Consistent-Field Calculations for Diazo Systems

Robin Challoner,* Robin K. Harris,*,† and John A. Tossell‡

*Department of Chemistry, University of Durham, South Road, Durham DH1 3LE, United Kingdom; and ‡Department of Chemistry and Biochemistry, University of Maryland, College Park, Maryland 20742

Received April 15, 1996; revised January 27, 1997

An off-magic-angle spinning study of the nonassociated molecular solid, doubly ^{15}N-labeled 5-methyl-2-diazobenzenesulphonic acid hydrochloride (I) is reported. The validity of the off-magic-angle spinning approach under fast-spinning conditions is verified by average Hamiltonian theory. Ab initio SCF calculations were performed on the simpler molecule, $C_6H_5N_2^+$, to provide the shielding parameters, the dipolar coupling between the two nitrogen nuclei, and the electric field gradient existing at both the α-nitrogen and β-nitrogen sites. The calculated values are in good agreement with the shielding and effective dipolar coupling data elucidated in the present investigation, and with a previous study of the two singly ^{15}N-labeled isotopomers in which information concerning the electric field gradient at the α and β sites was deduced.

INTRODUCTION

The determination of shielding and dipolar tensor information from the nuclear magnetic resonance spectra of homonuclear spin-pair systems to provide information concerning both molecular structure and dynamics has resulted from developments based on sophisticated magic-angle spinning NMR experiments (*1*). However, the pioneering work in this area was performed on small doubly ^{13}C-labeled molecules enclathrated in an argon matrix at 15 K (*2*). It was demonstrated that the observed powder patterns depended intimately on the mutual orientation of the shielding and dipolar tensors, which exhibit a fixed geometric relationship for all molecules. Moreover, the dipolar vector is well defined in the molecular frame, and so spectral analysis yields the orientation of the shielding tensors relative to that frame. This approach has since been extended via two-dimensional methods as a means of determining the above-mentioned spin parameters with even greater accuracy (*3*).

Under MAS conditions, average Hamiltonian theory (AHT) (*4*) demonstrates that, for homonuclear spin-pair systems, an anisotropic second-order perturbation term, which is dependent on the difference between the shielding tensor orientations as well as the magnitude of the dipolar coupling, contributes to the spectrum to promote broadening of the isotropic spectral features (*5*). Phenomenologically, this may be visualized as a consequence of the mutual spin flips between the two nuclei interrupting the coherent averaging process of MAS by producing changes in the local field experienced at a given nucleus during the rotor period. This effect tends to be maximized under conditions of slow spinning for the situation where the two shielding tensors are symmetry-related but far from colinear. The complex and unusual lineshapes observed under these conditions (*6*) do not lend themselves to a straightforward interpretation in the manner of the spectral analysis for the static sample. For the case where a large isotropic shift difference exists between the two nuclei, the influence of the second-order perturbation term tends to be truncated, although that of the dipolar coupling may be reintroduced by adjusting to the rotational resonance condition ($\omega_{iso}^{\Delta} = n\omega_r$) whereby the spinning frequency, or a submultiple of the spinning frequency, is matched to the difference in isotropic shifts of the two nuclei (*7*). Under this condition, striking spectral features are observed, which, for the case of vanishing shift anisotropy, may be interpreted in terms of powder distributions based on the nonsecular contributions of the dipolar interaction for $n = 1, 2$. In the presence of shielding anisotropy, however, highly complex spectral features are observed which would arguably benefit from an analysis based on Floquet theory (*8*).

Here, we demonstrate, using an AHT approach, that off-magic-angle spinning (OMAS) under conditions of fast sample rotation offers a route to a simplified analysis in these cases. The fast sample rotation is a requirement to ensure that the Hamiltonian describing the system may be expressed only in terms of the quantities that commute with each other during the rotor cycle, so that the time evolution of the system can be expressed in a closed form. The large isotropic

† To whom correspondence should be addressed.

1090-7807/97 $25.00

shift difference for the two nuclei ensures that the spectrum associated with a given crystallite orientation may always be described as first order for small deviations from the magic angle, thus aiding spectral simulation. The spectrum obtained for a homonuclear spin pair under OMAS conditions is very sensitive to the relative orientations of the dipolar and shielding tensors. Using such a method, we extract the relevant spin parameters for the ^{15}N pair present in doubly ^{15}N-labeled 5-methyl-2-diazobenzenesulphonic acid hydrochloride (**I**),

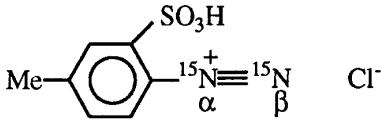

for which the two nitrogen nuclei exhibit markedly different chemical shifts. Moreover, the high degree of ''local'' symmetry enables an estimation of the orientations of the various tensor interactions relative to the molecular frame to be made, which assists in the spectral interpretation. Furthermore, we note that the diazo moiety behaves as a model for the application of this experiment to the azo linkage found in pigments based on phenylazo-2-naphthols, which participate in keto-hydrazo/enolazo tautomerism to which the internuclear nitrogen separation is sensitive.

The experimental values for the principal components of the shielding tensors extracted for the above-mentioned compound using the OMAS method are compared with the calculated values for the model compound $C_6H_5N_2^+$ derived from a random-phase approximation (RPA) localized orbital/local origin (LORG) method (*9*) in which the resultant expressions for a given shielding tensor may be decomposed into intrinsic bond and lone-pair contributions. The centroid of charge of the localized orbitals is used as the origin for the calculation of shielding, but with all localized molecular orbitals whose centroids reside within 0.9 Å of the nitrogen nucleus of interest (viz. one core and four valence MOs) ''pulled'' onto the nitrogen nucleus for shielding evaluation. Good agreement is obtained between the experimental and calculated principal components of the shielding tensor.

Ab initio SCF calculations were performed to estimate the electric field gradients existing at both the α-nitrogen and β-nitrogen sites, which were then compared with the values obtained from an experimental study of the two singly ^{15}N-labeled compounds using a combination of static and MAS experiments (*10*). Again, good agreement is obtained between theory and experiment.

EXPERIMENTAL

All measurements were performed on a Chemagnetics CMX200 spectrometer using a double air-bearing probe and frequencies of 200.13 and 20.28 for the ^1H and ^{15}N nuclei, respectively. A sample of doubly ^{15}N-labeled (20%) ammonium nitrate was used to set the Hartmann–Hahn match for the ^{15}N and ^1H radiofrequency channels. The nitrate resonance of this compound was used to set the angle in the off-magic-angle spinning experiment. The nitrate resonance was also used to reference the shieldings relative to the ^{15}N resonance in nitromethane.

The OMAS lineshape was calculated using a Q Basic program with processing in Microsoft Excel. After calculating the frequencies of the singularities for the $m = +\frac{1}{2}$ and $m = -\frac{1}{2}$ eigenstates of the neighboring ^{15}N nucleus as discussed below, the powder patterns corresponding to each distinct neighboring ^{15}N eigenstate were calculated and the results co-added.

THEORY

Consider the Hamiltonian of the homonuclear spin pair modulated by sample spinning in the high-field approximation (*12*)

$$\begin{aligned} H(t)/\hbar &= [H_z(t) + H_d(t) + H_J]/\hbar \\ &= -\omega_k(t)I_z^k - \omega_l(t)I_z^l + \omega_d(t)[I_z^kI_z^l \\ &\quad - \tfrac{1}{4}(I_+^kI_-^l + I_-^kI_+^l)] + \omega_J[I_z^kI_z^l \\ &\quad + \tfrac{1}{2}(I_+^kI_-^l + I_-^kI_+^l)], \end{aligned} \quad [1]$$

where $\omega_k(t)$ and $\omega_l(t)$ are the instantaneous Zeeman angular frequencies of the two spins k and l, and $\omega_d(t)$ and ω_J represent the dipolar and J couplings between the spins. All equations are in angular frequency units. We may rewrite the Hamiltonian [1] in terms of composite frequencies

$$\begin{aligned} H(t)/\hbar &= [H_\Sigma(t) + H_\Delta(t) + H_A(t) + H_B(t)]/\hbar \\ &= -\tfrac{1}{2}\Sigma(t)(I_z^k + I_z^l) - \tfrac{1}{2}\Delta(t)(I_z^k - I_z^l) \\ &\quad + 2A(t)I_z^kI_z^l + \tfrac{1}{2}B(t)(I_+^kI_-^l + I_-^kI_+^l), \end{aligned} \quad [2]$$

where

$$\begin{aligned} \Sigma(t) &= \omega_k(t) + \omega_l(t) \\ \Delta(t) &= \omega_k(t) - \omega_l(t) \\ A(t) &= \tfrac{1}{2}(\omega_d(t) + \omega_J) \\ B(t) &= \tfrac{1}{2}(-\omega_d(t) + 2\omega_J). \end{aligned} \quad [3]$$

Following a pulse, the FID is given by

$$S(t) = \mathrm{tr}\{\rho(t)I_+\} = \mathrm{tr}\{I_+U(t)I_-U(t)^\dagger\}, \quad [4]$$

where $U(t)$ is the time-evolution propagator

$$U(t) = T\exp\left[-i\int_0^t dt' H(t')\right] \quad [5]$$

with T the Dyson time-ordering operator.

The time-evolution propagator may be expressed as

$$U(t) = U_\Sigma(t)U_A(t)U_{\Delta+B}(t), \quad [6]$$

where

$$U_\Sigma(t) = \exp\left[-i\int_0^t dt' H_\Sigma(t')\right]$$

$$U_A(t) = \exp\left[-i\int_0^t dt' H_A(t')\right]$$

$$U_{\Delta+B}(t) = T\exp\left\{-i\int_0^t dt'[H_\Delta(t') + H_B(t')]\right\}. \quad [7]$$

The time-ordering operator T is not relevant for $U_\Sigma(t)$ and $U_A(t)$ because $H_\Sigma(t)$ and $H_A(t)$ are inhomogeneous interactions. The propagator $U_{\Delta+B}(t)$, which includes the time-ordering operator T, cannot usually be represented in an analytical form, but if the condition $\|H_\Delta + H_B\| \ll \omega_R$ holds, then we may apply AHT (*4*) to estimate $U_{\Delta+B}(t)$ (*12*). In first order, this propagator may be approximated by

$$U_{\Delta+B}(t_R) = \exp[-i\bar{H}^{(0)}_{\Delta+B}t_R], \quad [8]$$

where

$$\bar{H}^{(0)}_{\Delta+B} = \frac{1}{t_R}\int_0^{t_R} dt'[H_\Delta(t') + H_B(t')] \quad [9]$$

and the cycle time for the application of AHT is the rotor period $t_R = 2\pi/\omega_R$. The propagators $U_\Sigma(t)$ and $U_A(t)$ are given by straightforward time averages because rotor synchronization of the sampling was assumed in the AHT approach.

Thus,

$$\begin{aligned} S(t_R) = {} & (1 - \sin 2\theta)\exp[-i\{\tfrac{1}{2}(\bar{\Sigma} + \bar{R}) + \bar{A}\}t_R] \\ & + (1 + \sin 2\theta)\exp[-i\{\tfrac{1}{2}(\bar{\Sigma} + \bar{R}) - \bar{A}\}t_R] \\ & + (1 + \sin 2\theta)\exp[-i\{\tfrac{1}{2}(\bar{\Sigma} - \bar{R}) + \bar{A}\}t_R] \\ & + (1 - \sin 2\theta)\exp[-i\{\tfrac{1}{2}(\bar{\Sigma} - \bar{R}) - \bar{A}\}t_R], \end{aligned} \quad [10]$$

where

$$\bar{R} = \sqrt{\bar{\Delta}^2 + \bar{B}^2}, \quad \sin 2\theta = \bar{B}/\sqrt{\bar{\Delta}^2 + \bar{B}^{-2}} \quad [11]$$

and

$$\begin{aligned} \bar{\Sigma} &= \bar{\omega}_k + \bar{\omega}_l \quad \bar{\Delta} = \bar{\omega}_k - \bar{\omega}_l \\ \bar{A} &= \tfrac{1}{2}\omega_J + \tfrac{1}{2}\bar{\omega}_d \quad \bar{B} = \omega_J - \tfrac{1}{2}\bar{\omega}_d \end{aligned} \quad [12]$$

with

$$\begin{aligned} \bar{\omega}_k &= \bar{\omega}_k^{iso} + \tfrac{1}{2}(3\cos^2\theta^s - 1) \\ &\quad \times [\tfrac{1}{2}\omega_0^k\Delta_\sigma^k\{(3\cos^2\beta - 1) + \eta^k\sin^2\beta\cos 2\alpha\}] \\ \bar{\omega}_l &= \bar{\omega}_l^{iso} + \tfrac{1}{2}(3\cos^2\theta^s - 1) \\ &\quad \times [\tfrac{1}{2}\omega_0^l\Delta_\sigma^l\{(3\cos^2\beta - 1) + \eta^l\sin^2\beta\cos 2\alpha\}] \\ \bar{\omega}_d &= -\tfrac{1}{2}(3\cos^2\theta^s - 1)(3\cos^2\beta - 1)D, \end{aligned} \quad [13]$$

where D is the dipolar coupling constant in angular frequency units.

Here we have assumed rotation about an arbitrary axis inclined at θ^s with respect to the magnetic field. Furthermore, we have assumed that the interactions are diagonal in the molecular frame and that the dipolar vector is colinear with the principal components of the two shielding tensors. Extension of the equations to remove this assumption is feasible, but the results are likely to be too cumbersome for general use and are not necessary for the case considered here. The tensor transformation from the molecular frame (MOL), through the rotor axis system (ROT) to the laboratory frame (LAB) was considered:

$$\text{MOL} \xrightarrow{(\alpha,\ \beta,\ \gamma)} \text{ROT} \xrightarrow{(\omega_r t,\ \theta^s,\ 0)} \text{LAB}. \quad [14]$$

Equation [10] tells us that four spectral lines are obtained for a given crystallite orientation, in analogy with an *AB* *J*-coupled solution-state NMR spectrum. However, in the present instance, the fast-spinning ^{15}N CPMAS spectrum of doubly ^{15}N-labeled 5-methyl-2-diazobenzene sulphonic acid hydrochloride reveals that the isotropic J coupling between the two nuclei is either zero or close to zero. Thus, here the spectral splittings arise as a consequence of the influence of the scaled dipolar coupling, which nevertheless may contain a contribution from the anisotropy in J.

Under slower spinning conditions, it is necessary to analyze the influence of higher-order average Hamiltonian terms. To second order, the propagator $U_{\Delta+B}(t)$ may be approximated by

$$U_{\Delta+B}(t_R) = \exp[-i(H^{(0)}_{\Delta+B} + H^{(1)}_{\Delta+B})t_R], \quad [15]$$

where

$$H^{(1)}_{\Delta+B} = \frac{-i}{2t_R}\int_0^{t_R} dt' \,[H(t'), \int_0^{t'} dt'' \, H(t'')] \quad [16]$$

$$= \frac{i}{2} K'[I^k_+ I^l_- - I^k_- I^l_+] \quad [17]$$

$$K' = \frac{1}{\omega_R}(-C_1'^{\Delta} S_1'^{B} + S_1'^{\Delta} C_1'^{B} - \tfrac{1}{2} C_2'^{\Delta} S_2'^{\Delta} + \tfrac{1}{2} S_2'^{\Delta} C_2'^{B}) \quad [18]$$

with $C_i'^{\lambda}$, $S_i'^{\lambda}$ ($\lambda = \Delta, B$; $i = 1, 2$) defined by the coefficients of the dynamic parts of the difference Hamiltonian of the anisotropic shielding constants, $H_{\Delta}(t)$, and the flip-flop Hamiltonian of the dipolar coupling, $H_B(t)$, modulated by sample spinning. We have neglected the terms which vanish after taking a powder average.

Thus,

$$\begin{aligned} S(t_R) &= (1 - \sin 2\eta \cos\epsilon)\exp[-i\{\tfrac{1}{2}(\bar{\Sigma} + \bar{Q}) + \bar{A}\}t_R] \\ &+ (1 + \sin 2\eta \cos\epsilon)\exp[-i\{\tfrac{1}{2}(\bar{\Sigma} + \bar{Q}) - \bar{A}\}t_R] \\ &+ (1 + \sin 2\eta \cos\epsilon)\exp[-i\{\tfrac{1}{2}(\bar{\Sigma} - \bar{Q}) + \bar{A}\}t_R] \\ &+ (1 - \sin 2\eta \cos\epsilon)\exp[-i\{\tfrac{1}{2}(\bar{\Sigma} - \bar{Q}) - \bar{A}\}t_R], \end{aligned} \quad [19]$$

where

$$\begin{aligned} \bar{Q} &= \sqrt{\bar{\Delta}^2 + \bar{B}^2 + K'^2} \\ \sin 2\eta &= (\bar{B} + K'^2)/\sqrt{\bar{\Delta}^2 + \bar{B}^2 + K'^2} \\ \cos\epsilon &= \bar{B}/\sqrt{\bar{B}^2 + K'^2}. \end{aligned} \quad [20]$$

The FID has a form similar to that in Eq. [10] with the exception that, for a given crystallite orientation, the K' term introduces a frequency shift and an intensity correction for the four spectral lines. The significance of the spectral influence of K' is diminished at faster spinning frequencies. Under slower spinning conditions, the K' term renders the spectrum spinning-frequency dependent.

RESULTS AND DISCUSSION

The OMAS spectrum of doubly ^{15}N-labeled 5-methyl-2-diazobenzenesulphonic acid hydrochloride is shown in Fig. 1a for rotation at 6.4 kHz about an axis inclined at 57.3° with respect to the magnetic field. The scaling factor associated with the Legendre polynomial is thus −0.062 as separately determined from the scaling of the shielding anisotropy associated with the ^{15}N nitrate resonance in doubly ^{15}N-labeled ammonium nitrate. Figure 1 reveals powder-pattern features in the regions of each of the isotropic shifts associated with the two ^{15}N CPMAS sites in the molecule, namely the α-nitrogen resonance at −150.5 ppm and the β-nitrogen resonance at −62.6 ppm. The two powder-pattern features are well separated on account of the small deviation from the magic angle and the large isotropic shift difference between the two nitrogen nuclei, which may be accounted for by the fact that the molecular structure of the diazo compound is normally drawn with a formal positive charge on the α nitrogen and a lone pair of electrons on the β nitrogen.

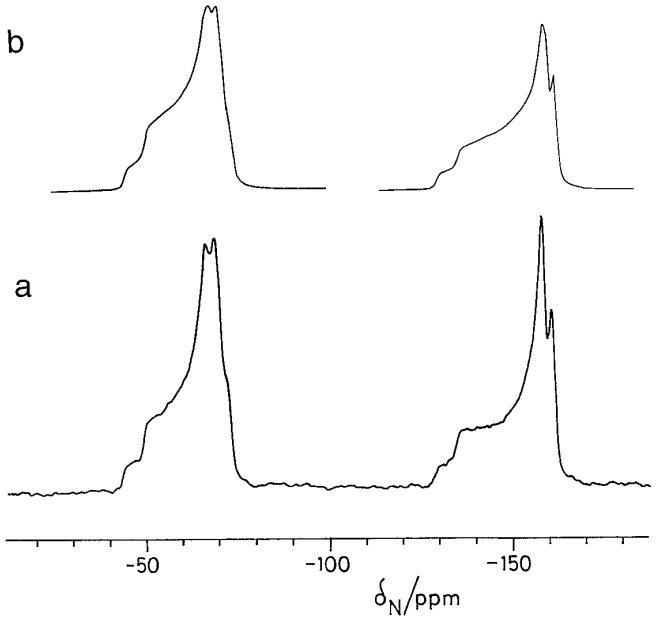

FIG. 1. The OMAS ^{15}N CPMAS spectrum ($\theta^s = 57.3°$) of 5-methyl-2-diazobenzene sulphonic acid hydrochloride. (a) Experimental spectrum obtained at a spinning frequency of 6.4 kHz. A total of 720 free-induction decays were accumulated under cross-polarization conditions using a contact time of 8 ms and a recycle delay of 20 s. (b) Simulations of the powder patterns. The simulations reveal that the α-^{15}N shielding tensor is axially symmetric, but the β-^{15}N shielding tensor is not. A 12 Hz Lorentzian line broadening was used in each case.

With the assumption that the relevant nuclear spin interactions are diagonal in the molecular frame and, moreover, that the dipolar vector is colinear with the two ^{15}N shielding tensors, Eqs. [10] and [13] demonstrate that in the fast-spinning limit we may represent the orientational dependence of the spectral angular frequency for a given crystallite orientation as

$$\frac{\omega^{k,l}}{\omega_0^{k,l}\Delta_\sigma^{k,l}} = \frac{1}{2}(3\cos^2\theta^s - 1)\left[\frac{1}{2}\left(1 - \frac{2mD'}{\omega_0^{k,l}\Delta_\sigma^{k,l}}\right) \times (3\cos^2\beta - 1) + \frac{\eta^{k,l}}{2}\sin^2\beta\cos 2\alpha\right] \quad [21]$$

with the further assumption that $\bar{\Delta}$ dominates the expressions for the spectral intensity and frequency in Eq. [11]. This assumption is justified by the large difference in isotropic shifts of the two ^{15}N nuclei relative to the magnitude of the scaled dipolar interaction. θ^s is the angle of inclination of the rotation axis with respect to the magnetic field, $\Delta\sigma$ and η are the anisotropy and asymmetry in the shielding, β and α are the two Euler angles required to align the shielding tensors relative to the rotation axis, β is also the Euler angle describing the relationship between the dipolar vector and the rotation axis, and $D' = (D - \Delta J/3)$, with ΔJ the anisotropy in the J tensor (the unique component of which is assumed to be colinear with the dipole vector). The quantum number m may take the values $+\frac{1}{2}$ and $-\frac{1}{2}$ with equal probability. The fast-spinning frequency regime was confirmed by variable-spinning-frequency experiments.

In the absence of a dipolar interaction/anisotropy in J contribution, the discontinuities associated with a full powder distribution occur (in units of $\omega^{k,l}/\omega_0^{k,l}\Delta_\sigma^{k,l}$) at $-\frac{1}{2}(1 + \eta^{k,l})$, $-\frac{1}{2}(1 - \eta^{k,l})$, and unity, and correspond to $\sigma_{yy}^{k,l}$, $\sigma_{xx}^{k,l}$, and $\sigma_{zz}^{k,l}$, respectively. However, the above equation illustrates that the influence of the dipolar interaction/anisotropy in J contribution is to split each discontinuity into a doublet corresponding to the two possible and equally likely values of m. In particular, the σ_{zz} component of the shielding tensor is split into a doublet of separation $2DP_2(\cos\theta^s)$, whereas the discontinuities associated with the σ_{yy} and σ_{xx} are split into doublets of separation $DP_2(\cos\theta^s)$. Thus, the powder patterns observed in the regions of each of the isotropic shifts in Fig. 1 may be considered as the coaddition of two powder patterns (subspectra) corresponding to the two eigenstates of the ^{15}N nucleus. With the further assumption that the expressions for the spectral intensity are dominated by the large isotropic shift difference term, the two powder patterns make an equivalent contribution to the spectral intensity. Thus, the fine structure associated with the α nitrogen in Fig. 1 immediately reveals an axially symmetric shielding tensor, whereas the fine structure associated with the β nitrogen indicates a nonaxially symmetric shielding tensor.

The colinearity of the dipolar vector with the two ^{15}N shielding tensors is confirmed by the simulations shown in Fig. 1b. A value of 920 ± 20 Hz was obtained for the effective dipolar coupling constant, D', while for the two

TABLE 1
Nitrogen-15 Shielding Tensor Data[a]

Molecule		σ_{zz}	σ_{yy}	σ_{xx}	$\Delta\sigma$	η	σ_{iso}
I[b]	N_α	314.2	−133.3	−133.3	447.5	0	15.9
	N_β	176.2	−166.8	−229.8	374.5	0.25	−73.5
II[c]	N_α	393.4	−132.1	−136.0	527.5	0.01	41.8
	N_β	206.9	−162.8	−231.4	404.0	0.25	−62.4
N_2[d]		337.2	−266	−266	603.2	0	−64.9

[a] All principal components of shielding refer to an absolute scale in ppm. The experimentally obtained shielding values were converted to this scale by assuming an absolute ^{15}N shielding in nitromethane of −135.8 ppm.
[b] Experimental values from this study.
[c] Ab initio SCF calculation (RPA LORG).
[d] Reported values for solid molecular nitrogen at ''0K'' [Ref. (*18*)].

^{15}N shielding tensors the following principal components of the shielding tensors were obtained (using the convention $|\sigma_{zz} - \sigma_{iso}| > |\sigma_{xx} - \sigma_{iso}| > |\sigma_{yy} - \sigma_{iso}|$): For the α nitrogen, $\sigma_{zz} - \sigma_{ref} = 450 \pm 2$ ppm, $\sigma_{yy} - \sigma_{ref} = \sigma_{xx} - \sigma_{ref} = 2.5 \pm 2$ ppm, the asymmetry parameter, η, is equal to zero, and the shielding anisotropy, $\sigma_{zz} - \langle\sigma_{yy} + \sigma_{xx}\rangle = 448$ ppm; for the β nitrogen, $\sigma_{zz} - \sigma_{ref} = 312 \pm 2$ ppm, $\sigma_{yy} - \sigma_{ref} = -31 \pm 2$ ppm, and $\sigma_{xx} - \sigma_{ref} = -94 \pm 2$ ppm. The shielding anisotropy for the β nitrogen is equal to 375 ppm and $\eta = 0.25$. The colinearity of the dipolar vector with the ^{15}N β-nitrogen shielding tensor ensures that the observed spectrum is invariant to the orientation of σ_{yy} and σ_{xx} in the XY molecular plane.

To aid the interpretation of these data, ab initio SCF calculations were performed on the simpler model molecule, $C_6H_5N_2^+$ (**II**):

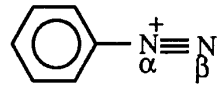

The lone-pair electrons at nitrogen ensure that ^{15}N chemical shifts are more difficult to calculate than those for a nucleus such as carbon, given the potential for lone-pair interactions with electron deficient moieties. The geometry of $C_6H_5N_2^+$ was first optimized in C_{2v} symmetry at the SCF level using a 6-31 G* basis (*13*) and the program GAMESS (*14*) to obtain a C–N bond distance of 1.415 Å and a N–N bond distance of 1.077 Å. The N–N bond distance implies a dipolar coupling of 988 Hz and is in good agreement with a distance of 1.103 ± 0.008 Å estimated from the experimental effective dipolar coupling. For this optimized geometry of $C_6H_5N_2^+$, the ^{15}N shielding tensors were calculated using the RPA LORG (*9*) method as implemented in the program RPAC (*15*) with a 6-31G** basis on the N, C, and H atoms. The calculated absolute shieldings in ppm are given in Table 1. For comparison, an absolute shielding of 256.8 ppm for

TABLE 2
The Effect of Basis Set Size and Correlation to the Nitrogen Shieldings in the Methyl Diazonium Ion, $CH_3N_2^+$

	σ^N (ppm)		
	N_α	N_β	σ^{N_α}-σ^{N_β}
LORG (6-31G**)	34.1	−58.2	92.3
LORG (6-31G (2*d*,*p*))	34.8	−55.1	89.9
SOLO (6-31G**)	64.9	−10.4	75.3

NH_3 at the 6-31G* SCF-optimized geometry using a 6-31G** LORG basis was obtained, which compares with the estimate of 264.54 ppm derived from spin rotation constants and other ab initio calculations (*16*). The experimentally determined principal components of the shielding tensors are also given in Table 1 and were converted to the absolute shielding scale previously established by investigations of a number of small, ^{15}N-labeled molecules by using an absolute shift for ^{15}N in nitromethane of −135.8 ppm (*17*). Previously reported data for $^{15}N_2$ were also converted to this scale (*18*). It is immediately apparent that the calculated principal components of the shielding tensors are in rather good agreement with the experimentally determined values, particularly so in the cases of the σ_{xx} and σ_{yy} components. The calculated σ_{zz} components are both more strongly shielded than the experimentally determined values, which presumably arises as a consequence of the discrepancy in the actual and calculated internuclear nitrogen separation. However, the calculations indicate that both the α nitrogen and the β nitrogen are strongly shielded along the N−N vector in agreement with the experiment. The calculated asymmetry parameters are in remarkably good agreement with the experimental values, the α nitrogen being almost axially symmetric, whereas the β nitrogen shows considerable departure from axial symmetry. The shielding parameters for molecular nitrogen at ''0K'' show the same essential feature as the calculated values except that both nitrogens exhibit axially symmetric shielding tensors in this case, because of the $C_{\infty v}$ symmetry of the nitrogen molecule. Furthermore, the orientations of the calculated ^{15}N shielding tensors relative to the molecular frame reinforce the notion of colinearity of the relevant interactions as deduced from experimental results.

The influence of basis set size and correlation on the isotropic shifts for the α and β nitrogens was investigated by calculations performed on the methyl diazonium ion, $CH_3N_2^+$ using 6-31G* optimized geometry. The results are indicated in Table 2. The 6-31G (2*d*, *p*) basis has two 3*d* polarization functions on the C and N, rather than one as in the 6-31G** basis. It is apparent that the effect of doubling the 3*d* functions is very small. This is in contrast to the results obtained by the second-order LORG (SOLO) method, which incorporates electron correlation. This changes the absolute shieldings of the two nitrogen sites substantially, but the shielding difference is only slightly reduced.

The strong shielding along the N−N vector may be rationalized by considering the paramagnetic contribution to the shielding from the N−N bond. The expression for this contribution may be developed from a molecular orbital approach using a linear combination of atomic orbitals, which reveals that the shielding component along a given axis is primarily determined by the circulation of electrons in a plane perpendicular to the axis and containing the nucleus (*19*). Thus, σ^p_{zz} is determined mainly by the $1\pi_u(x) \rightarrow 1\pi^*_g(y)$ and $1\pi_u(y) \rightarrow 1\pi^*_g(x)$ transitions, which are of significantly higher energy than the $2\sigma_g \rightarrow 1\pi^*_g(y)$ and $1\pi_u(y) \rightarrow 2\sigma^*_u$ transitions which determine σ^p_{xx}, and the $2\sigma_g \rightarrow 1\pi^*_g(x)$ and $1\pi_u(x) \rightarrow 2\sigma^*_u$ transitions which determine σ^p_{yy}. The significantly higher energy of the $\pi_u \rightarrow \pi^*_g$ transitions relative to the $2\sigma_g \rightarrow 1\pi^*_g$ and $1\pi_u \rightarrow 2\sigma^*_u$ transitions (which are similar in energy) ensures that σ^p_{zz} is significantly more shielded than σ^p_{xx} and σ^p_{yy}. Moreover, σ^p_{xx} and σ^p_{yy} are predicted to be similarly shielded, as observed experimentally. Furthermore, the experimentally determined shielding parameters for both the α nitrogen and the β nitrogen are in excellent agreement with a study of the singly ^{15}N-labeled analogues of the diazo moiety obtained under static conditions (*10*).

The difference in shielding of the α nitrogen and the β nitrogen in $C_6H_5N_2^+$ was investigated by analyzing the contributions of the various localized molecular orbitals to the calculated isotropic shifts for the two nitrogen nuclei. The results are shown in Table 3. It is apparent that the β nitrogen is substantially deshielded by its σ lone pair plus a slightly increased deshielding from the N−N π orbitals.

The effective dipolar coupling of 920 ± 20 Hz for the two ^{15}N nuclei obtained from this work is in excellent agreement with a value of 905 ± 11 Hz reported by an earlier rotational resonance study (*11*). In that case, the effective dipolar coupling was deduced from the widths of the highly structured sideband resonances that occurred under rotational-resonance conditions. Such features are a reflection of the sizeable shielding anisotropies associated with both

TABLE 3
Contributions to σ^N (ppm) from the 6-31G LORG Calculation on $C_6H_5N_2^+$ from Individual Localized Molecular Orbitals**

	σ^N (ppm)	
Localized molecular orbital	N_α	N_β
C−N_α σ	−80	−28
N_β σ lone pair	−38	−128
N_α−N_β σ	−25	−37
N_α−N_β π	−16, −17	−45, −46

TABLE 4
Quadrupolar ^{14}N Data[a]

Molecule	Atoms(s)	eq_{xx}	eq_{yy}	eq_{zz}	χ	η
I[b]	N_α	—	—	0.41	−1.40	0.39
	N_β	—	—	1.16	−4.01	0.46
II[c]	N_α	−0.2588	−0.0892	0.3480	−1.20	0.49
	N_β	−0.2637	−0.7621	1.0258	−3.53	0.49
N_2[d]		—	—	1.35	−4.65	0

[a] The electric field gradient components are given in atomic units, whereas the quadrupole coupling constants, χ, are given in megahertz.

[b] Experimental values from previous study [Ref. (*10*)]. The asymmetry parameters were obtained from an NQR analysis [Ref. (*20*)].

[c] Ab initio SCF calculation.

[d] Reported values for solid molecular nitrogen at 4.2 K [Ref. (*21*)].

^{15}N nuclei, in addition to anisotropy in the effective dipolar coupling.

Ab initio SCF calculations were also performed to obtain the electric field gradient existing at both of the nitrogen sites of the simple model $C_6H_5N_2^+$. The results are shown in Table 4, as are the calculated quadrupole coupling constants (χ) for a ^{14}N nucleus at either site, assuming a quadrupole moment of 0.015×10^{-28} m^{-2} for ^{14}N. The calculated values of −1.20 and −3.53 MHz for the α and β nitrogens in $C_6H_5N_2^+$ are in good agreement with the experimental values of −1.40 and −4.01 MHz determined for singly ^{15}N-labeled 5-methyl-2-diazobenzenesulphonic acid hydrochloride by a combination of ^{15}N static and CPMAS measurements (*10*). The calculated asymmetry parameters for both ^{14}N sites are in reasonable agreement with a previous NQR analysis (*20*). Thus, the calculated values are in agreement with the field gradient, eq_{zz}, for the α nitrogen being about one-third of that of the β nitrogen. The increase in the magnitude of the quadrupole coupling of the β nitrogen relative to that of the α nitrogen points to a predominant canonical form of type **III,**

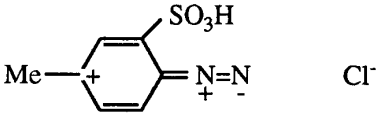

where the α nitrogen is *sp*-hybridized and the β nitrogen sp^2 hybridized, the *s*-orbital part contributing nothing to the quadrupole coupling. The Sternheimer anti-shielding correction was neglected for the calculated electric field gradients, since it makes no more than an estimated 10% correction in the present case. We note that the β-nitrogen quadrupole coupling constant is closest in magnitude to that reported for solid N_2 at 4.2 K (*21*).

CONCLUSION

An OMAS approach has been used to characterize the shielding and dipolar coupling parameters for the ^{15}N spin pair present in the doubly ^{15}N-labeled compound, 5-methyl-2-diazobenzenesulphonic acid hydrochloride under fast-spinning conditions. The shielding parameters, the dipolar coupling between the nitrogen nuclei, and the electric field gradient existing at both the α-nitrogen and the β-nitrogen sites [obtained from an earlier study of both singly ^{15}N-labeled compounds (*10*)] were compared with the calculated values from ab initio SCF calculations using the RPA LORG method (*9*) on the simpler molecule $C_6H_5N_2^+$ and found to be in good agreement.

The OMAS method circumvents the need for sophisticated simulations of the highly complex sideband lineshapes that occur under rotational resonance conditions to obtain the same information. The approach is made more straightforward in the present case by the use of fast magic-angle spinning. Under slower-spinning conditions, the K' term makes a spectral contribution which manifests itself practically as the distortion of the features observed under fast-spinning conditions. We note that the technique is particularly relevant in the present case given that at slower spinning frequencies the situation may be regarded as an offset from the rotational resonance conditions such that, to some extent, mutual spin flips between the two ^{15}N nuclei during the rotor period tend to mix the shielding anisotropies associated with the two nuclei, so that erroneous conclusions would result from the analysis of the sideband manifold identified with each ^{15}N site, whereas at faster spinning frequencies, the sideband intensities are too small to allow an accurate analysis.

ACKNOWLEDGMENTS

We thank the U.K. Engineering and Physical Sciences Research Council for financial support under Grant GR/H96096, and also Paul Jonsen for his involvement with the synthesis of the isotopically enriched material.

REFERENCES

1. M. G. Colombo, B. H. Meier, and R. R. Ernst, *Chem. Phys. Lett.* **146,** 189 (1988); D. P. Raleigh, M. H. Levitt, and R. G. Griffin, *Chem. Phys. Lett.* **146,** 71 (1988); R. Tycko and G. Dabbagh, *Chem. Phys. Lett.* **173,** 461 (1990); J. H. Ok, R. G. S. Spencer, A. E. Bennett, and R. G. Griffin, *Chem. Phys. Lett.* **197,** 389 (1992); A. E. Bennett, J. H. Ok, S. Vega, and R. G. Griffin, *J. Chem. Phys.* **96,** 8624 (1992); D. K. Sodickson, M. H. Levitt, S. Vega, and R. G. Griffin, *J. Chem. Phys.* **98,** 6742 (1992).
2. K. W. Zilm and D. M. Grant, *J. Am. Chem. Soc.* **103,** 2913 (1980).
3. M. Linder, A. Höhener, and R. R. Ernst, *J. Chem. Phys.* **73,** 4959 (1980); W. E. J. R. Maas, A. P. M. Kentgens, and W. S. Veeman, *J. Chem. Phys.* **87,** 6854 (1987); T. Nakai, J. Ashida, and T. Terao, *J. Chem. Phys.* **88,** 6049 (1988).
4. U. Haeberlen, *in* ''High Resolution NMR in Solids: Selective Averaging, Advances in Magnetic Resonance'' (J. S. Waugh, Ed.), Suppl. 1, Academic Press, New York, 1976; U. Haeberlen and J. S. Waugh, *Phys. Rev.* **175,** 453 (1968).
5. M. M. Maricq and J. S. Waugh, *J. Chem. Phys.* **70,** 3300 (1979).
6. A. Kubo and C. A. McDowell, *J. Chem. Phys.* **93,** 7156 (1990).

7. M. H. Levitt, D. P. Raleigh, F. Creuzet, and R. G. Griffin, *J. Chem. Phys.* **92,** 6347 (1990).
8. A. Schmidt and S. Vega, *J. Chem. Phys.* **96,** 2655 (1992).
9. A. E. Hansen and T. D. Bowman, *J. Chem. Phys.* **82,** 5033 (1985).
10. R. Challoner and R. K. Harris, *Solid State NMR* **4,** 65 (1995).
11. R. Challoner and R. K. Harris, *Chem. Phys. Lett.* **228,** 589 (1994).
12. T. Nakai, R. Challoner, and C. A. McDowell, *Chem. Phys. Lett.* **180,** 13 (1991); R. Challoner, T. Nakai, and C. A. McDowell, *J. Chem. Phys.* **94,** 7038 (1992).
13. W. J. Hehre, L. Radom, P. von R. Schleyer, and J. A. Pople, ''Ab initio Molecular Orbital Theory,'' Wiley, New York, 1986.
14. M. W. Schmidt, K. K. Baldridge, J. A. Boatz, S. T. Elkert, M. S. Gordon, J. H. Jensen, S. Koseki, N. Matsunaga, K. A. Nguyen, S. J. Su, T. L. Windus, M. Du Puis, and J. A. Montgomery, *J. Comput. Chem.* **14,** 1347 (1993).
15. A. E. Hansen, B. Voight, and S. Rettup, *Int. J. Quant. Chem.* **23,** 595 (1983); T. D. Bowman and A. E. Hansen, RPAC Molecular Properties Package, Version 9.0, Southern Illinois Univ., 1991.
16. S. G. Kukolich, *J. Am. Chem. Soc.* **97,** 5704 (1975).
17. C. J. Jameson, A. K. Jameson, D. Oppusunggu, S. Wille, P. M. Burrell, and J. Mason, *J. Chem. Phys.* **74,** 81 (1982).
18. T. M. Duncan, ''A Compilation of Chemical Shift Anisotropies,'' Farragut Press, Madison, Wisconsin, 1990.
19. J. A. Pople, *J. Chem. Phys.* **37,** 53 (1962); M. Sardashti and G. E. Maciel, *J. Phys. Chem.* **92,** 4620 (1988).
20. J. Stephenson and J. A. S. Smith, personal communication.
21. F. W. Terran and T. A. Scott, *Bull. Am. Phys. Soc. Ser. II,* **3,** 23 (1958).